ACS APPLIED MATERIALS & INTERFACES

Research Article

www.acsami.org

Asphalt-Derived High Surface Area Activated Porous Carbons for Carbon Dioxide Capture

Almaz S. Jalilov,[†,⊥] Gedeng Ruan,[†,⊥] Chih-Chau Hwang,[†] Desmond E. Schipper,[†] Josiah J. Tour,[†] Yilun Li,[†] Huilong Fei,[†] Errol L. G. Samuel,[†] and James M. Tour*[,†,‡,§]

[†]Department of Chemistry, [‡]Richard E. Smalley Institute for Nanoscale Science and Technology, and [§]Department of Materials Science and NanoEngineering, Rice University, 6100 Main Street, Houston, Texas 77005, United States

Supporting Information

ABSTRACT: Research activity toward the development of new sorbents for carbon dioxide (CO_2) capture have been increasing quickly. Despite the variety of existing materials with high surface areas and high CO_2 uptake performances, the cost of the materials remains a dominant factor in slowing their industrial applications. Here we report preparation and CO_2 uptake performance of microporous carbon materials synthesized from asphalt, a very inexpensive carbon source. Carbonization of asphalt with potassium hydroxide (KOH) at high temperatures (>600 °C) yields porous carbon materials (**A-PC**) with high surface areas of up to 2780 $m^2\ g^{-1}$ and high CO_2 uptake performance of 21 mmol g^{-1} or 93 wt % at 30 bar and 25 °C. Furthermore, nitrogen doping and reduction with hydrogen yields active N-doped materials (**A-NPC** and **A-rNPC**) containing up to 9.3% nitrogen, making them nucleophilic porous carbons with further increase in the Brunauer–Emmett–Teller (BET) surface areas up to 2860 $m^2\ g^{-1}$ for **A-NPC** and CO_2 uptake to 26 mmol g^{-1} or 114 wt % at 30 bar and 25 °C for **A-rNPC**. This is the highest reported CO_2 uptake among the family of the activated porous carbonaceous materials. Thus, the porous carbon materials from asphalt have excellent properties for reversibly capturing CO_2 at the well-head during the extraction of natural gas, a naturally occurring high pressure source of CO_2. Through a pressure swing sorption process, when the asphalt-derived material is returned to 1 bar, the CO_2 is released, thereby rendering a reversible capture medium that is highly efficient yet very inexpensive.

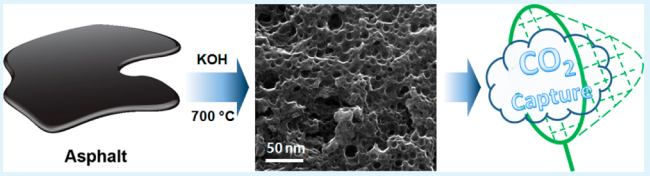

KEYWORDS: *asphalt, CO_2 capture, porous carbonaceous materials, carbonization, nitrogen addition*

INTRODUCTION

Global climate change is the main environmental concern that might be directly affected by anthropogenic carbon dioxide (CO_2) emission sources, which include industrial power plants, refineries, and natural gas wells, the last having CO_2 contents that can range from 1 to 70 mol % depending on the region of the world.[1,2] Therefore, efficient and reversible CO_2 capture from flue gas or from the higher pressure natural gas wells remains important in the use of carbon fuels if we are to maintain high standards of environmental stewardship, or the so-called "green carbon" approach.[3−6] In the sorption processes, in addition to the highly used aqueous amine solvents and membrane technologies, solid sorbents such as activated carbon, zeolites and, more recently, metal organic frameworks (MOFs) are promising alternative materials for capturing CO_2.[7−9] Despite the many new solid sorbents developed in past years, cost remains a dominant factor when it comes to choosing the ultimate material.

Within CO_2 capture technologies, compression and separation of CO_2 at high pressures, high flow rates and low partial pressures of CO_2 remains a challenge for next-generation solid sorbents. Although aqueous amine solutions are among the most common industrial processes for CO_2 capture,[10] the process is corrosive and energy intensive due to the high energy requirements for regeneration of the amines, and their large space requirements exclude off-shore use. Solid sorbents are promising alternative technologies for CO_2 capture,[8] and they project several advantages over conventional separation technologies. These include lower energy regeneration requirements, higher capacity and selectivity, and easier handling of the noncorrosive solids.[8] Generally, lower heat capacities, faster kinetics of sorption and desorption, and mechanical strength of solid sorbents are the primary advantages of solid sorbents for the use of pressure swing methods of CO_2 gas separation.[11,12]

An advantage of the meso- and microporous activated carbon materials over the other solid sorbents are the low cost of raw materials. The availability of a wide variety of carbon sources (e.g., coals, polymeric materials, coke pitch, wood, biomass, and industrial byproducts) makes activated carbons cost-effective at the industrial production stage. Recently, we reported porous carbon materials synthesized from sulfur and nitrogen containing polymers. These afforded sulfur and nitrogen-containing porous carbons, **SPC** and **NPC**, respectively, which showed superior CO_2 uptake at higher pressures and greater CO_2/CH_4 gas separation selectivity relative to the most

Received: December 15, 2014
Accepted: December 22, 2014
Published: December 22, 2014

DOI: 10.1021/am508858x
ACS Appl. Mater. Interfaces 2015, 7, 1376−1382

common solid sorbents such as activated carbon, zeolites and MOFs.[13]

Here we report template free[14,15] synthesis and characterization of activated porous carbons from asphalt, which serves as a very inexpensive carbon source, and the synthesis is done in one step. In general, the structure of asphalt is complex, which mainly consists of asphaltenes, the toluene or benzene soluble portion of crude asphalt.[16,17] Asphaltenes contains nanosized conjugated aromatic domains that are linked by small aliphatic side chains with heteroatom containing-polar functional groups, which induces van der Waals, hydrogen bonding and charge-transfer interactions to form porous asphaltene aggregates.[18,19] Therefore, activation of crude asphalt formed micro- and mesoporous carbon materials that have high surface areas, which could be further activated by nitrogen impregnation, to yield activated porous carbons with even higher CO_2 uptake performances than **SPC** and **NPC**.

RESULTS AND DISCUSSION

Synthesis and Characterization of Porous Materials. Porous carbons were prepared by carbonization of mixtures of asphalt and potassium hydroxide (KOH) at elevated temperatures under inert atmosphere (Ar). The treatment of asphalt with KOH was performed at various temperatures (200−800 °C) and different asphalt:KOH weight ratios (varied from 1:1 to 1:4). The CO_2 uptake performance of the final porous carbon materials (Figures S1 and S2, Supporting Information) was evaluated based upon the parameter changes in the synthesis. The asphalt-derived porous carbon is designated as **A-PC**. The highest surface area **A-PC** was synthesized at 700 °C (Scheme 1) with a weight ratio of asphalt:KOH = 1:4 (Figure S1, Supporting Information).

Scheme 1. Synthesis of Highest Surface Area A-PC

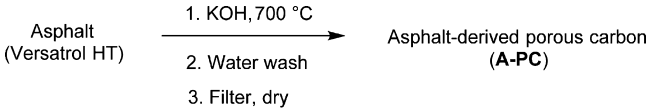

As shown in Figure 1, **A-PC** has a steep nitrogen uptake at low pressures (0−0.3 P/P_o), and has a typical type IV sorption isotherm, indicating meso-porosity of the material (Figure 1, inset). The Brunauer−Emmett−Teller (BET) surface area (2780 $m^2\ g^{-1}$) and the pore volume (1.17 $cm^3\ g^{-1}$) were calculated from the nitrogen isotherms (Table 1). X-ray photoelectron spectroscopy (XPS) of the **A-PC** showed C 1s and O 1s signals, with ~10% oxygen content, assigned to C—O and C═O functional groups (Figure S3, Supporting Information).

Scanning electron microscopy (SEM) images of the **A-PC** show porous material with a uniform distribution of the pores, as shown in Figure 2. Uniform distribution of the pores is further indicated by the transmission electron microscopy (TEM) image (Figure 2b) with pore diameters >2 nm. This is close to the values determined from the nitrogen absorption isotherms.

Treatment of **A-PC**s with NH_3 at elevated temperatures resulted in asphalt-derived N-impregnated porous carbon materials (**A-NPC**). The nitrogen content (3−9% from 0%) and the surface area 2860 $m^2\ g^{-1}$ increased after treatment of **A-PC**s with NH_3 at higher temperatures (Figure S4, Supporting Information), as shown in Tables 1 and 2. This leads to the

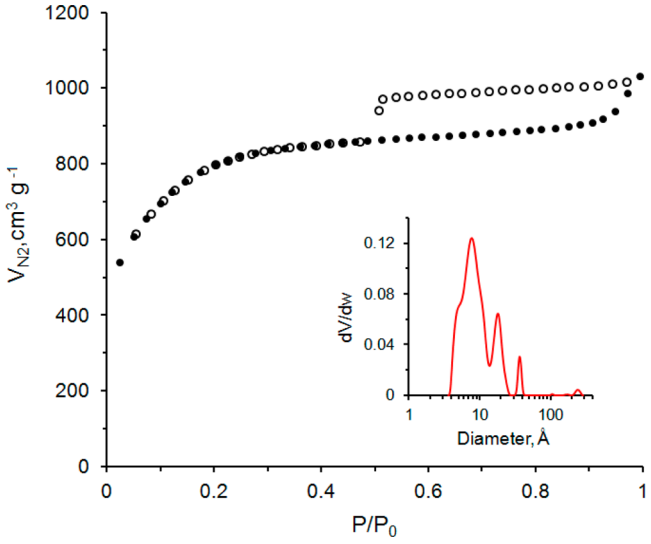

Figure 1. Nitrogen sorption isotherms for **A-PC** at 77 K. Absorption (filled symbols) and desorption (empty symbols). Inset: differential nonlocal density functional theory (NLDFT) pore size distributions curve.

Table 1. Properties and CO_2 Uptake Performances of Activated Porous Carbons

samples	S_{BET} ($m^2\ g^{-1}$)[a]	pore volume ($cm^3\ g^{-1}$)[a]	density (g cm^{-3})	CO_2 uptake capacity at 30 bar[b]	
				mmol g^{-1}	wt %
A-PC	2780	1.17	1.78	21.1	93
A-NPC	2860	1.20	2.00	23.8	104
A-rNPC	2580	1.09	2.10	26.0	114
SPC	2500	1.01	2.21	18.4	81
NPC	1490	1.40	1.8	14.7	65
rNPC[c]	1450	1.43	1.8	16.8	74

[a]Estimated from N_2 absorption isotherms at 77 K; samples dried at 200 °C for 20 h prior to the measurements. [b]CO_2 uptake at 23 °C. [c]Prepared by H_2 reduction of **NPC** at 600 °C.[13]

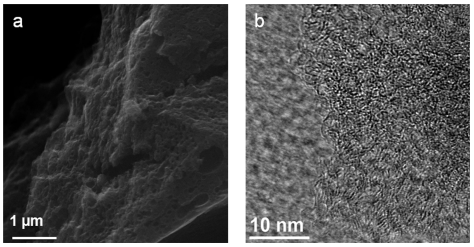

Figure 2. (a) SEM and (b) TEM images of the **A-PC**.

modified porous material of up to 9.3% N concentration obtained at 800 °C. At lower NH_3 treatment temperatures, the content of nitrogen decreased proportionally, reaching 2.7% at 500 °C (Table 2).

The surface N-bonding configurations reveal three main nitrogen functional groups in the surface of the carbon framework. As shown in Figure 3, the XPS N 1s spectra at variable doping temperatures deconvoluted into three peaks with binding energies at 399.0, 400.7, and 401.7 eV. These are in the range of typical binding energies corresponding to pyridinic N, pyrollic N, and graphitic N, respectively. While

DOI: 10.1021/am508858x
ACS Appl. Mater. Interfaces 2015, 7, 1376−1382

Table 2. Elemental Composition and CO_2 Uptake Performances of Activated Porous Carbons That Were Aminated with NH_3 at 500—800 °C

	XPS						CO_2 uptake capacity at 30 bar[b]	
samples[a]	C%	O%	N%	pyridinic N%	pyrrolic N%	graphitic N%	mmol g^{-1}	wt %
A-NPC(500)	91.1	6.1	2.7	29.7	63.3	7.0	23.2	102
A-NPC(600)	90.6	6.4	3.0	33.1	52.6	14.3	23.2	102
A-NPC(700)	91.1	4.2	4.7	53.2	41.4	5.4	23.8	104
A-NPC(800)	81.0	9.7	9.3	52.3	45.4	2.3	20.9	92
A-rNPC	88.0	7.5	4.5	55.1	40.3	4.6	26.0	114

[a]The temperature of amination is shown in parentheses. [b]CO_2 uptake at 23 °C.

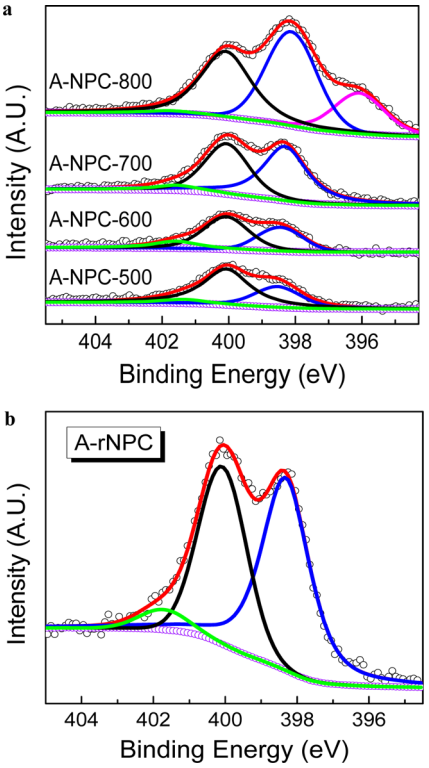

Figure 3. High-resolution XPS N 1s spectra of the (a) **A-NPC** formed at various NH_3 treatment temperatures, and (b) **A-rNPC** formed after reduction with H_2 at 700 °C. Experimental data are the open circles and the fitted curves are the solid lines.

lower temperature (500 °C) NH_3 treatment primarily leads to pyrollic type functional groups, treatment at higher temperatures (800 °C) results in pyridinic and graphitic nitrogens.[20] The new peak at a binding energy of 396.0 was observed at 800 °C, which is assigned to the N−Si binding energy. It is likely that at higher pyrolysis temperatures, silica-doping from the quartz tube occurs, which also results in lower CO_2 uptake (Table 2). Further H_2 treatment of **A-NPC** at 700 °C with the intent of reducing the amines resulted in the reduced porous carbon material (**A-rNPC**). The elemental composition and the surface area of the **A-rNPC** were investigated using XPS (Figure 3b and Table 2). There is noticeable change in the graphitic nitrogen signal after the H_2 reduction of **A-NPC**, which decreased from 5.4% to 4.6% and an increase in the concentration of the pyridinic nitrogen signal from 53.2% to 55.1% (Table 2). This suggests the H_2-induced transformation of graphitic nitrogen to the pyridinic nitrogen (Scheme 2). The proposed mechanistic pathway for H_2 reductive N−C bond cleavage is shown in Figure S5, eq 1 (Supporting Information).

Scheme 2. Conversion of Graphitic Nitrogen into Pyridinic Nitrogen during the Reduction with H_2

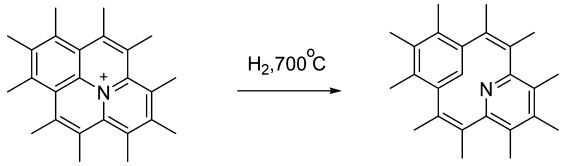

An increase in the basic character of the nitrogen functional groups would be anticipated due to the H_2 reduction of the pyridinic nitrogens to aliphatic nitrogens (Figure S5, eq 2, Supporting Information); however, we were not able to detect an increase in the pyrrolic nitrogen content during the H_2 reduction. Instead, the H_2 reduction could be contributing to the changes in the pore structures, which leads to the decrease in the BET surface area. Because the nitrogen sorption isotherms did change considerably during both the N-impregnation and reduction processes (Figure S6, Supporting Information), we conclude that such activation has substantial effect on the morphological parameters of the porous carbons. Similar behavior was observed during the activation of porous carbons with NH_3, where the authors of that study explained the observed increase in the surface area by the reaction between the carbon lattice and NH_3 to afford an evolution of methane. The gaseous evolution can increase the surface area.[21] Schematic representation of the synthetic route for the **A-rNPC** is shown in Scheme 3.

CO_2 Uptake. Activated carbons with a wide variety of surface parameters including surface area, pore structure and active sites on the surface, have been widely used as gas sorbents. **SPC** and **NPC** were prepared from the carbonization of poly[(2-hydroxymethyl)thiophene] and poly(acrylonitrile), respectively.[13] **SPC** and **NPC** showed high CO_2 uptake 18.4 mmol g^{-1} (82 wt %) and 14.7 mmol g^{-1} (65 wt %) (Table 1), respectively; comparable or better than conventional solid sorbents such as activated carbons, zeolites and MOFs.[13] Shown in Figure 4 are the CO_2 uptake of the activated porous carbons from asphalt (**A-PC**, **A-NPC**, and **A-rNPC**) along with the **SPC**, **NPC**, and commercial activated carbon (**AC**), measured by the volumetric method at room temperature over the pressure range 0 to 30 bar. 30 bar was chosen as the upper pressure limit from the approximation that a 300 bar natural gas well-head pressure containing ~10% CO_2 has 30 bar partial pressure of CO_2. Volumetric CO_2 uptakes show little hysteresis, which suggests the reversible nature of CO_2 uptake of the materials. No degradation of the porous carbons is observed during the CO_2 sorption−desorption process from 0 to 30 bar (Figure S7, Supporting Information) or over 8 cycles (Figure S8, Supporting Information). CO_2 uptake at a pressure

DOI: 10.1021/am508858x
ACS Appl. Mater. Interfaces 2015, 7, 1376−1382

Scheme 3. Schematic Illustration of the Preparation of A-NPC and A-rNPC

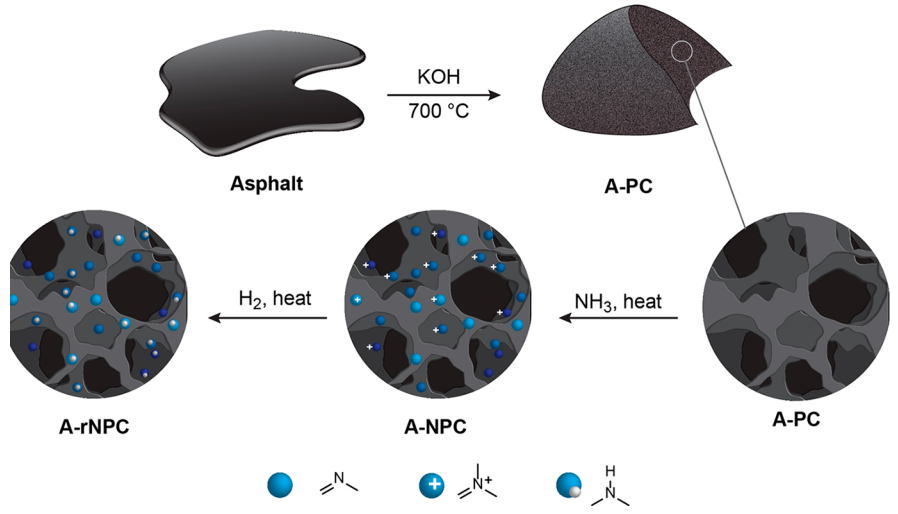

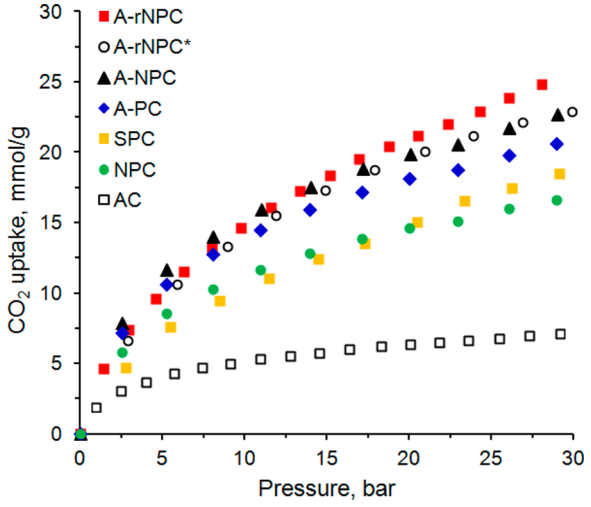

Figure 4. Comparison of volumetric and gravimetric CO_2 uptake of **A-PC**, **A-NPC** and **A-rNPC** with the other porous carbon sorbents at 23 °C. An asterick indicates gravimetrically performed absolute CO_2 uptake of **A-rNPC** at 25 °C (Figures S9−S11, Supporting Information).

of 30 bar are given in Tables 1 and 2, and the uptake capacities are up to 26 mmol g^{-1} (114 wt %), which are not only the highest reported among the activated carbons[22−24] but also comparable with MOFs used under similar conditions.[25−28] Unlike MOFs, these can be prepared at a much lower cost and in one or two thermalization steps from asphalt.

A-rNPC has the highest CO_2 uptake performance at 30 bar, although the highest surface area is obtained for **A-NPC**. The volumetric uptake measurements correlate with the gravimetric uptake measurements (Figures 4, S9−S11, Supporting Information). As we increase the N-impregnation temperature (from 100 to 800 °C, Figure S4, Supporting Information), the nitrogen content starts to increase gradually, which affects the CO_2 uptake performance of the **A-NPC**s (Table 2). Thus, we conclude that the basic nitrogen functional groups (pyridinic and pyrrolic) are essential for the enhanced CO_2 uptake performance of the porous carbon material. At lower NH_3 treatment temperatures, the concentration of the pyrrolic nitrogens increases while pyridinic nitrogens decrease (Table 2). These results indicated that the pyrolysis temperature during the NH_3 treatment is one of the critical factors in determining the CO_2 uptake performance.

Figure 5 shows the high and low pressure CO_2 uptake of **A-rNPC** as the temperature increases. As in other solid sorbents

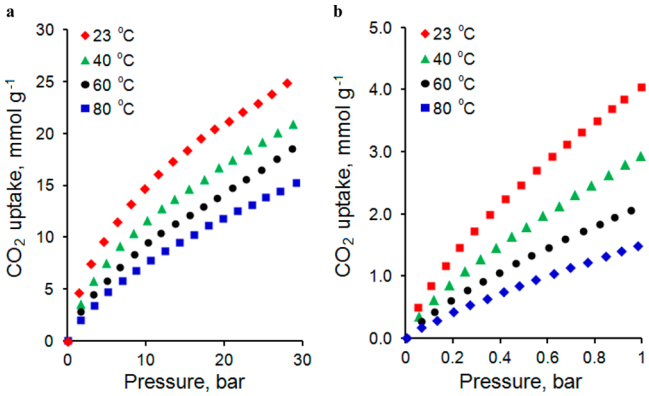

Figure 5. Volumetric uptake of CO_2 on **A-rNPC** as a function of temperature. (a) Higher pressure range of 0 to 30 bar; (b) lower pressure range of 0 to 1 bar.

such as activated carbons, zeolites and MOFs, the capacity decreases with increasing temperature. However, when compared with commercial activated carbon and **SPC**, the **A-rNPC** has a greater CO_2 uptake at higher temperatures.

One of the key properties of the solid sorbents is their CO_2/CH_4 selectivity. CO_2:CH_4 selectivity in this paper is defined as the molar ratios of sorbed CO_2 and CH_4 (ν_{CO2}/ν_{CH4}). In order to evaluate the CO_2:CH_4 selectivity of **A-PC**, **A-NPC** and **A-rNPC**s, we compared CH_4 uptake performances with **SPC**, activated carbon and ZIF-8 sorbents at 23 °C. Figure 6 shows the comparison of the CO_2 and CH_4 sorption capacities of **A-rNPC** and **SPC**. **A-rNPC** has higher CH_4 (8.6 mmol g^{-1}) uptake relative to **SPC** (7.7 mmol g^{-1}) at 30 bar, although both **A-rNPC** and **SPC** have similar apparent surface areas of 2580 m^2 g^{-1} and 2500 m^2 g^{-1}, respectively. The molar ratios of sorbed CO_2 and CH_4 (ν_{CO2}/ν_{CH4}) were estimated by the ratios of the amount of the absorbed gases at 30 bar, which was highest for **A-rNPC** (3.0), as compared to values for **SPC** (2.6), activated carbon (1.5) and ZIF-8 (1.9).[13]

DOI: 10.1021/am508858x
ACS Appl. Mater. Interfaces 2015, 7, 1376−1382

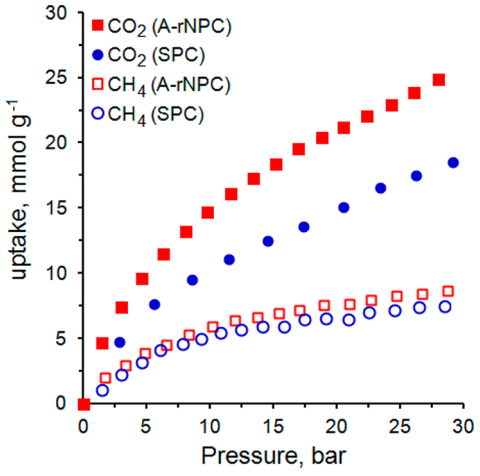

Figure 6. Volumetric CO_2 (filled symbols) and CH_4 (empty symbols) uptake of **A-rNPC** (red) and **SPC** (blue) at 23 °C.

The isosteric heat of absorption (Qst) of CO_2 and CH_4 on the surfaces of **A-PC** and **A-rNPC** were calculated using low pressure CO_2 sorption isotherms at 0 and 23 °C, as shown in Figure 7. The values for absorption of CH_4 were found to be

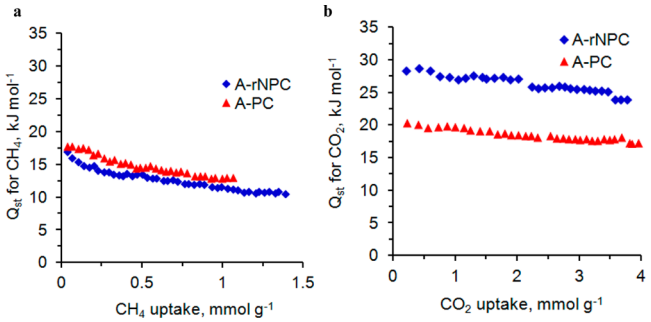

Figure 7. Isostreric heat of absorption (Qst) using (a) CH_4 and (b) CO_2 on **A-PC** and **A-rNPC** at 0 and 23 °C.

comparable for **A-PC** and **A-rNPC** at 17 to 20 kJ mol^{-1} (Figure 7a), and they have relatively constant values during the filling of the pores. This points to the nucleophilic sites that can interact with CO_2 but that do not have strong interactions with sorbed CH_4 molecules.[13] The observed values of 17 to 20 kJ mol^{-1} are close to the reported values for the absorption of methane on MOFs (MIL-53, 17.0 kJ mol^{-1})[29] and zeolites (NaY, 17−17.8 kJ mol^{-1})[30] and are all above the liquefaction enthalpy of methane (8.2 kJ mol^{-1}). Contrarily, the absorption energies of CO_2 changes considerably between **A-PC** (20 kJ mol^{-1}) and **A-rNPC** (29 kJ mol^{-1}), as seen in Figure 7b, which is indicative of the stronger interactions between nitrogen containing nucleophilic sites of the pores in **A-rNPC** with the CO_2 molecules. During the increase in the filling of the pores, the CO_2 absorption enthalpy of **A-PC** starts to decrease and eventually reaches the enthalpy of liquefaction of CO_2 (17.2 kJ mol^{-1}) (Figure 7b), while **A-rNPC** reaches its lowest value at 24 kJ mol^{-1} (Figure 7b). Relatively weak enthalpy for **A-PC**, in contrast to the previously reported **SPC** (57 kJ mol^{-1}), suggests a better reversible CO_2 uptake performance of undoped **A-PC** for the more efficient removal of CO_2 at low pressures, in comparison to the nitrogen doped **A-rNPC** and sulfur containing **SPC**. Higher sorption enthalpy for the sulfur containing **SPC** than **A-rNPC** points to the stronger interactions of nucleophilic sulfur-containing sites of the pores with CO_2 molecules. It is also worthy to mention that the **SPC** and **A-rNPC** have smaller CH_4 sorption selectivity in comparison to the CO_2 sorption selectivity (Figure 6). This points to a weak interaction of CH_4 with the sulfur and nitrogen functional groups in the pores. CO_2 has a larger quadrupole moment (13.4 C m^2) than does the CH_4 (nonpolar).

CONCLUSION

In summary, we have demonstrated the successful synthesis of microporous active carbon from asphalt with uniform distribution of pore sizes and the subsequent activation with nitrogen functional groups. Changing the preparation conditions, the porous materials possess variable surface areas and nitrogen contents. Activated porous carbons from asphalt have been shown to have CO_2 uptake of 26 mmol g^{-1} (114 wt %), which is the highest for any porous carbons and also one of the highest among all the porous materials. Additionally, nitrogen functionalized microporous carbon materials exhibit greater CO_2:CH_4 than the nucleophilic porous materials prepared from the heteroatom-containing organic polymers. These observations indicate the porous materials from asphalt are promising and very inexpensive sorbents for industrial applications where CO_2 is removed from natural gas streams.

EXPERIMENTAL SECTION

Materials. Versatrol HT, Versatrol M, Asphasol Supreme and Natural asphalt from Chile were kindly provided by MI SWACO, a Schlumberger Company. Untreated Gilsonite and Untreated Gilsonite Substitute are both provide by Prince Energy. Activated carbon Darco G-60 and KOH were used as received from Sigma-Aldrich.

Synthesis of Asphalt Derived Porous Carbon (A-PC). 0.50 g of asphalt (Versatrol HT) and 1.50 g (26.7 mmol) of KOH were mixed well in a mortar.[13] The mixture was heated on a quartz boat inserted within a quartz tube furnace at 700 °C for 1 h with Ar flow at 500 sccm, 1 atm, before being permitted to cool to room temperature. Then the product was washed thoroughly with DI water and acetone until the filtrate attained pH 7. The **A-PC** powder was dried in an oven at 100 °C until a constant weight was achieved to afford 0.22 g of **A-PC**. Under comparable conditions different types of asphalt were screened: natural asphalt from Chile, Versatrol M, Asphasol Supreme, Untreated Gilsonite and Untreated Gilsonite Substitute; Figure S12 (Supporting Information) shows the comparative CO_2 uptake data. Moreover, higher CO_2 uptake was reached by preliminary pretreatment of Versatrol M for 2 h at 400 °C and then activating at 800 °C for 1 h (Figure S13, Supporting Information). Also, increasing the asphalt:KOH ratio to 1:5 and the temperature of the pretreatment to 750 °C for Natural asphalt, increased CO_2 uptake (Figure S14, Supporting Information).

Synthesis of Nitrogen Doped Asphalt Derived Porous Carbon (A-NPC) and Reduced Nitrogen Doped Asphalt Derived Porous Carbon (A-rNPC). 0.20 g of **A-PC** powder was placed in a quartz boat and transferred into to a quartz tube furnace. The powder was heated at 700 °C for 1 h with NH_3 flow at 100 sccm, 1 atm, before cooling to room temperature to afford 0.17 g of **A-NPC.** To synthesize **A-rNPC**, 0.20 g of **A-NPC** powder was heated at 700 °C for 1 h with H_2 flow at 100 sccm and Ar flow at 200 sccm at 1 atm to afford 0.18 g of **A-rNPC**.

Volumetric Sorption. Volumetric sorption measurements of CO_2 or CH_4, or premixed gas were carried out in an automated Sievert instrument[13] (Setaram PCTPro). Typically, ~120 mg of sorbent was placed in a stainless steel sample cell and pretreated at 150 °C for 2 h under vacuum (~20 mTorr). The sample volume was calibrated by helium before the sorption measurement.

Gravimetric Sorption. Gravimetric sorption measurements of CO_2 were carried out in a Rubotherm magnetic suspension balance[31]

DOI: 10.1021/am508858x
ACS Appl. Mater. Interfaces 2015, 7, 1376−1382

(Rubotherm, Germany). A blank test without sample was used to measure the weight and volume of the empty sample holder. For a typical measurement, ~120 mg of sorbent was placed in the sample holder and pretreated at 150 °C for 2 h under vacuum (~20 mTorr). A buoyancy test with helium was then used to measure the sample weight and sample volume before the sorption measurement.

Characterization. The XPS were obtained on a PHI Quantera SXM scanning X-ray microprobe system using a 100 μm X-ray beam of which the takeoff angle was 45° and pass energy was 140 eV for the survey and 26 eV for the high resolution elemental analysis. The surface areas, pore volumes and pore size distributions (Barrett–Joyner–Halenda, BJH) of different samples were obtained using an automated BET surface analyzer (Quantachrome Autosorb-3b). The samples were heated at 150 °C for 15 h under vacuum (20 mTorr) before each measurement. Scanning electron microscopy (SEM) images were taken at 20 keV in a FEI Quanta 400 high resolution field emission scanning electron microscope. High resolution transmission electron microscopy (TEM) images were obtained in a 2100F field emission gun transmission electron microscope. The porous carbon samples were transferred to a C-flat TEM grid (Protochips).

■ ASSOCIATED CONTENT

Supporting Information

Optimization of the asphalt:KOH ratio during the carbonization process, optimization of the temperature during the carbonization process, XPS of **A-PC**, optimization of the NH_3 treatment temperature during N-impregnation of **A-PC**, proposed mechanisms for high temperature H_2 reduction of **A-NPC**, nitrogen sorption isotherms for **A-PC**, **A-NPC**, and **A-rNPC**, CO_2 sorption–desorption cycle on the **A-NPC** over a pressure range from 0 to 30 bar at 23 °C, eight consecutive CO_2 sorption–desorption cycles on the **A-NPC** over a pressure range from 0 to 30 bar at 23 °C, gravimetric CO_2 uptake on **A-PC**, comparison of the volumetric and gravimetric CO_2 uptake for **A-PC** at 23 and 25 °C, gravimetric CO_2 uptake on the **A-rNPC**, volumetric CO_2 uptake of porous carbons derived from different asphalt sources over a pressure range from 0 to 30 bar at 23 °C, volumetric CO_2 uptake of porous carbons derived from Versatrol M under different activation conditions over a pressure range from 0 to 30 bar at 23 °C, and volumetric CO_2 uptake of porous carbons derived from natural asphalt under different activation conditions over a pressure range from 0 to 30 bar at 23 °C. This material is available free of charge via the Internet at http://pubs.acs.org.

■ AUTHOR INFORMATION

Corresponding Author

*J. M. Tour. E-mail: tour@rice.edu.

Author Contributions

⊥These authors contributed equally.

Notes

The authors declare no competing financial interest.

■ ACKNOWLEDGMENTS

This work was graciously funded by Apache Corporation. MI SWACO-Schlumberger and Prince Energy kindly provided the asphalt samples.

■ REFERENCES

(1) Yang, H.; Xu, Z.; Fan, M.; Gupta, R.; Slimane, R. B.; Bland, A. E.; Wright, I. Progress in Carbon Dioxide Separation and Capture: A Review. *J. Environ. Sci.* **2008**, *20*, 14–29.

(2) Golombok, M.; Nikolic, D. Assessing Contaminated Gas. *Hart's EP Mag.*, June **2008**, p73–p75.

(3) Haszeldine, R. S. Carbon Capture and Storage: How Green Can Black Be? *Science* **2009**, *325*, 1647–1652.

(4) Herzog, H. J. What Future for Carbon Capture and Sequestration? *Environ. Sci. Technol.* **2001**, *35*, 148A–153A.

(5) Mikkelsen, M.; Jorgensen, M.; Krebs, F. C. The Teraton Challenge: A Review of Fixation and Transformation of Carbon Dioxide. *Energy Environ. Sci.* **2010**, *3*, 43–81.

(6) Tour, J. M.; Kittrell, C.; Colvin, V. L. Green Carbon as a Bridge to Renewable Energy. *Nat. Mater.* **2010**, *9*, 871–874.

(7) Aaron, D.; Tsouris, C. Separation of CO_2 from Flue Gas: A Review. *Sep. Purif. Rev.* **2005**, *40*, 321–348.

(8) Choi, S.; Drese, J. H.; Jones, C. W. Adsorbent Materials for Carbon Dioxide Capture from Large Anthropogenic Point Sources. *ChemSusChem* **2009**, *2*, 796–854.

(9) D'Alessandro, D. M.; Smit, B.; Long, J. R. Carbon Dioxide Capture: Prospects for New Materials. *Angew. Chem., Int. Ed.* **2010**, *49*, 6058–6082.

(10) Rochelle, G. T. Amine Scrubbing for CO_2 Capture. *Science* **2009**, *325*, 1652–1654.

(11) Yang, R. T. *Adsorbents: Fundamentals and Applications*; Wiley Interscience: Hoboken, NJ, 2003.

(12) Yong, Z.; Mata, V.; Rodrigues, A. E. Adsorption of Carbon Dioxide at High Temperature—A Review. *Sep. Purifi. Technol.* **2002**, *26*, 195–205.

(13) Hwang, C.-C.; Tour, J. J.; Kittrell, C.; Espinal, L.; Alemany, L. B.; Tour, J. M. Capturing Carbon Dioxide as a Polymer from Natural Gas. *Nat. Commun.* **2014**, *5*, 3961–3968.

(14) Dutta, S.; Bhaumik, A.; Wu, K. C.-W. Hierarchically Porous Carbon Derived from Polymers and Biomass: Effect of Interconnected Pores on Energy Applications. *Energy Environ. Sci.* **2014**, *7*, 3574–3592.

(15) Gong, Y.; Wei, Z.; Wang, J.; Zhang, P.; Li, H.; Wang, Y. Design and Fabrication of Hierarchically Porous Carbon with a Template-free Method. *Sci. Rep.* **2014**, DOI: 10.1038/srep06349.

(16) Spiecker, P. M.; Gawrys, K. L.; Kilpatrick, P. K. Aggregation and Solubility Behavior of Asphaltenes and Their Subfractions. *J. Colloid Interface Sci.* **2003**, *267*, 178–193.

(17) Gawrys, K. L.; Kilpatrick, P. K. Asphaltenic Aggregates are Polydisperse Oblate Cylinders. *J. Colloid Interface Sci.* **2005**, *288*, 325–334.

(18) Strausz, O. P.; Peng, P.; Murgich, J. About the Colloidal Nature of Asphaltenes and the MW of Covalent Monomeric Units. *Energy Fuels* **2002**, *16*, 809–822.

(19) Groenzin, H.; Mullins, O. C.; Eser, S.; Mathews, J.; Yang, M. G.; Jones, D. Molecular Size of Asphaltene Solubility Fractions. *Energy Fuels* **2003**, *17*, 498–503.

(20) Pels, J. R.; Kapteijn, F.; Moulijn, J. A.; Zhu, Q.; Thomas, K. M. Evolution of Nitrogen Functionalities in Carbonaceous Materials During Pyrolysis. *Carbon* **1995**, *33*, 1641–1653.

(21) Luo, W.; Wang, B.; Heron, C. G.; Allen, M. J.; Morre, J.; Maier, C. S.; Stickle, W. F.; Ji, X. Pyrolysis of Cellulose under Ammonia Leads to Nitrogen-Doped Nanoporous Carbon Generated through Methane Formation. *Nano Lett.* **2014**, *14*, 2225–2229.

(22) Wang, Q.; Luo, J.; Zhong, Z.; Borgna, A. CO_2 Capture by Solid Adsorbents and Their Applications: Current Status and New Trends. *Energy Environ. Sci.* **2011**, *4*, 42–55.

(23) Wegrzyn, J.; Gurevich, M. Adsorbent Storage of Natural Gas. *Appl. Energy* **1996**, *55*, 71–83.

(24) Himeno, S.; Komatsu, T.; Fujita, S. High Pressure Adsorption Equilibria of Methane and Carbon Dioxide on Several Activated Carbons. *J. Chem. Eng. Data* **2005**, *50*, 369–376.

(25) Wang, Q. M.; Shen, D.; Bulow, M.; Lau, M. L.; Deng, S.; Fitch, F. R.; Lemcoff, N. O.; Semanscin, J. Metallorganic Molecular Sieve for Gas Separation and Purification. *Microporous Mesoporous Mater.* **2002**, *55*, 217–230.

(26) Millward, A. R.; Yaghi, O. M. Metal-Organic Frameworks with Exceptionally High Capacity for Storage of Carbon Dioxide at Room Temperature. *J. Am. Chem. Soc.* **2005**, *127*, 17998–17999.

DOI: 10.1021/am508858x
ACS Appl. Mater. Interfaces 2015, 7, 1376–1382

(27) Llewellyn, P. L.; Bourrelly, S.; Serre, C.; Vimont, A.; Daturi, M.; Hamon, L.; De Weireld, G.; Chang, J.-S.; Hong, D.-Y.; Hwang, Y. K.; Jhung, S. H.; Férey, G. High Uptakes of CO_2 and CH_4 in Mesoporous Metal-Organic Frameworks MIL-100 and MIL-101. *Langmuir* **2008**, *24*, 7245−7250.
(28) Furukawa, H.; Ko, N.; Go, Y. B.; Aratani, N.; Choi, S. B.; Choi, E.; Yazaydin, A. O.; Snurr, R. Q.; O'Keeffe, M.; Kim, J.; Yaghi, O. M. Ultrahigh Porosity in Metal-Organic Frameworks. *Science* **2010**, *239*, 424−428.
(29) Bourrelly, S.; Llewellyn, P. L.; Serre, C.; Millange, F.; Loiseau, T.; Ferey, G. Different Adsorption Behaviors of Methane and Carbon Dioxide in the Isotypic Nanoporous Metal Terephthalates MIL-53 and MIL-47. *J. Am. Chem. Soc.* **2005**, *127*, 13519−13521.
(30) Mentasy, L.; Woestyn, A. M.; Basaldella, E.; Kikot, A.; Zgrablig, G. High Pressure Methane Adsorption on NaX and NaY Zeolites with Different Si/Al Ratios. *Adv. Sci. Technol.* **1994**, *11*, 209−220.
(31) Saha, D.; Deng, S. Hydrogen Adsorption on Ordered Mesoporous Carbon Doped with Pd, Pt, Ni, and Ru. *Langmuir* **2009**, *25*, 12550−12560.

DOI: 10.1021/am508858x
ACS Appl. Mater. Interfaces 2015, 7, 1376−1382